OPTICAL REVIEW Vol. 5, No. 5 (1998) 320-325

Colorimetric Calibration of Video Cameras Using Two Color Constancy Models

Noriyuki SHIMANO

Faculty of Science and Engineering, Kinki University, 3-4-1, Kowakae, Higashi-osaka, Osaka, 577-8502 Japan

(Received April 28, 1998; Accepted June 30, 1998)

Colorimetric calibration of color imaging devices is important to realize device independent color reproductions. However the calibration for digital or video cameras is difficult because a color image is acquired for unknown objects under various unknown illuminants. An experiment was carried out based on two computational color constancy models, the finite-dimensional linear model and the spectral sharpening model, to estimate colorimetric values using image data of a color chart captured by video camera. We estimated the colorimetric values by using a single reference reflectance with known spectral reflectance in a color chart under an unknown illuminant. The accuracy was evaluated by color differences in CIELAB color space and was compared on three different color charts under three different illuminants including a fluorescent lamp. It was confirmed that the two computational models do not require prior knowledge of illuminants and surfaces. The finite-dimensional linear model gave more accurate results than the spectral sharpening model in the simulations and experiments.

Key words: colorimetric calibration, color reproduction, image acquisition, computational color constancy

1. Introduction

With the advance of digital imaging devices their colorimetric calibration is important to establish device independent color reproductions. A number of studies have been carried out to calibrate color scanners,[1-4] however, the calibration is difficult for digital or video cameras, because color images of unknown objects are captured under various unknown illuminations. If a target object and an illuminant could be known in advance, conventional regression methods[1,2] and direct mapping and interpolation methods[3,4] could be used. For video or digital cameras, the colorimetric values must be estimated using three sensor responses of an unknown object captured under an unknown illuminant. The computational color constancy models are one clue to solving this problem. The finite-dimensional linear models[5-8] for surface reflectances[9-11] and illuminants,[12] and the spectral sharpening model[13,14] are particularly useful among them.

It is well known that the surface reflectances recovered by the finite-dimensional linear model are only two dimensional approximations if three sensor responses under a single unknown illuminant are used.[5-8] Modeling the surfaces by only two dimensional vectors is too small to represent the richness of surface colors. Moreover D'Zmura and Iverson showed that it is impossible to recover surface reflectances represented by three dimensional basis vectors using three sensor responses under a single illuminant.[7,8] Therefore, several scene restrictions are assumed to recover the surface spectral reflectances which are represented by three dimensional vectors with trichromatic visual systems.[15-17]

Shimano[18,19] recently showed that if a color chart has a single reference reflectance with known spectral reflectance, then any set of basis vectors can be used to represent various illuminants, even though those basis vectors are not adequate to represent an illuminant, in order to recover surface spectral reflectance of a color chart. He also showed that a restricted set of eigen vectors obtained by principal component analysis (PCA) on the data set of a color chart can be used to represent the surface reflectances of different kinds of media. This finding is important because prior knowledge of surfaces and illuminants is not required to estimate colorimetric values through the use of image data of unknown objects taken under unknown illuminants. This fact has the same advantage as does the spectral sharpening model by Finlayson *et al.*,[13,14] since the model does not use the finite-dimensional linear model for surfaces and illuminants. However, very little work is currently available in the published literature on the performance of the two models. The purpose of the present study is to establish a colorimetric calibration method of a video camera under unknown illuminants by comparing the estimation accuracy of the two models using the image data of three different color charts captured under three different illuminants including a fluorescent lamp.

2. Estimation Models

The light reflected from an object's surface is decomposed into two additive components: the body reflection and the interface reflection, and this is called dichromatic reflection model.[20,21] The term surface reflectance in this paper represents the body reflection component. The surface spectral reflectances measured by a spectrophotometer in this experiment also represent the body reflection component. The wavelength region used in the estimation was 400 to 700 nm at 10 nm intervals.

2.1 Finite-Dimensional Linear Model

Spectral distributions of object colors and daylight illuminants are well represented by the linear combination of low dimensional basis vectors derived by PCA of sur-

E-mail: shimano@me2.kindai.ac.jp

faces[9–11] and illuminants,[12] respectively. Cohen was the first to discover the finite-dimensional linear model for surfaces,[9] and later Maloney[11] and Dannemiller[22] showed that three to four basis vectors provide good approximations when the effects of sensitivities of visual system were taken into account. Judd *et al.*[12] showed that the daylight illuminants are well modeled by a set of three basis vectors. Three dimensional representation for the surfaces and illuminants are used for the trichromatic visual system in the present study: a surface reflectance $R(\lambda)$ and illuminant $E(\lambda)$ can be expressed as a linear combination of three basis vectors of surfaces $R_i(\lambda)_{,i=1-3}$ and illuminants $E_j(\lambda)_{,j=1-3}$, respectively.

The three sensor responses, with spectral sensitivities $S_i(\lambda)_{i=R,G,B}$, for a reference reflectance $R_r(\lambda)$ are represented by a matrix form as

$$\boldsymbol{p}_r = A\boldsymbol{\varepsilon}\,, \tag{1}$$

where $A_{i,j}=\int_{vis} S_i(\lambda)E_j(\lambda)R_r(\lambda)d\lambda$ and bold face letter $\boldsymbol{p}_r$ and $\boldsymbol{\varepsilon}$ express a 3×1 vector for image data and the illuminant's weights, respectively. The column vectors of weights $\boldsymbol{\varepsilon}$ can be computed easily by inverse matrix of A. Then, we can obtain spectral radiant power distribution functions by the three dimensional representation. The surface spectral reflectance can be recovered using the estimated illuminant. Using the recovered spectral function $\hat{E}(\lambda)$, we obtain sensor responses $\boldsymbol{p}$ of the other colors as a matrix form

$$\boldsymbol{p}=B\boldsymbol{\sigma}\,, \tag{2}$$

where matrix element $B_{i,j}$ is given by $B_{i,j}=\int_{vis} S_i(\lambda)R_j(\lambda)\times\hat{E}(\lambda)d\lambda$. The elements of column vector $\boldsymbol{\sigma}$ represent weights for the surface reflectances. If B is nonsingular, we can easily obtain $\boldsymbol{\sigma}$ by inverse matrix of B. Using estimated $\boldsymbol{\sigma}$, we can determine the spectral distributions of the surface reflectances.

The author showed that the recovered surface reflectances were almost unchanged for different illuminations using the restricted sets of basis vectors for illuminants and surfaces: the surface spectral reflectances were recovered without prior knowledge of illuminants and surfaces.[18,19]

2.2 *Spectral Sharpening Model*[13,14]

The spectral sharpening model is based on the idea that if the spectral sensitivities of photosensors were transformed to sharpened spectral sensitivities such as delta-functions by a linear transformation, then the ratio of the sharpened sensor's response of a surface $R(\lambda)$ to that of a reference surface $R_r(\lambda)$ would be unchanged by changes in illuminants.[13,14] The following equation represents the relation:

$$\frac{\int E_u(\lambda)R(\lambda)T_S S(\lambda)d\lambda}{\int E_u(\lambda)R_r(\lambda)T_S S(\lambda)d\lambda}=\frac{\int E_c(\lambda)R(\lambda)T_S S(\lambda)d\lambda}{\int E_c(\lambda)R_r(\lambda)T_S S(\lambda)d\lambda}\,, \tag{3}$$

where $E_u(\lambda)$ and $E_c(\lambda)$ are an unknown and a canonical spectral radiant power distribution of illuminants, respectively. $T_S S(\lambda)$ represents the sharpened spectral sensitivities of three sensors $S(\lambda)$ transformed by the spectral sharpening 3×3 matrix T_s and bold face letter $S(\lambda)$ represents a $3\times N$ matrix with three spectral sensitivities of sensors as the row vectors, where N represents the number of sampling points over the visible wavelength. The equation represents three separate equations for each channel. If the color matching functions $X(\lambda)$, which is a $3\times N$ matrix comprised of the three CIE color matching functions as row vectors, were transformed by another sharpening matrix T_c to narrow over the same wavelength range as $T_S S(\lambda)$, we would have the next relation[14]

$$\frac{\int E_u(\lambda)R(\lambda)T_S S(\lambda)d\lambda}{\int E_u(\lambda)R_r(\lambda)T_S S(\lambda)d\lambda}=\frac{\int E_c(\lambda)R(\lambda)T_C X(\lambda)d\lambda}{\int E_c(\lambda)R_r(\lambda)T_C X(\lambda)d\lambda}\,, \tag{4}$$

Since T_S and T_C are constant over the wavelength, Eq. (4) can be rewritten as

$$\frac{T_S\boldsymbol{p}}{T_S\boldsymbol{p}_r}=\frac{T_C\boldsymbol{t}}{T_C\boldsymbol{t}_r}\,, \tag{5}$$

where $\boldsymbol{p}$ and $\boldsymbol{t}$ represent 3×1 column vector of sensor responses and tristimulus values for a surface reflectance $R(\lambda)$, respectively. $\boldsymbol{p}_r$ and $\boldsymbol{t}_r$ are sensor response and tristimulus value of a reference reflectance $R_r(\lambda)$, respectively. If we use a reference reflectance $R_r(\lambda)$ in a color chart under unknown illuminant $E_u(\lambda)$, then tristimulus values of surface reflectance $R(\lambda)$ of other colors in a scene can be estimated relative to the canonical illuminant $E_c(\lambda)$ from observed values $\boldsymbol{p}$, $\boldsymbol{p}_r$ and tristimulus values $\boldsymbol{t}_r$ of the reference reflectance under canonical illuminant provided spectral sharpening matrixes are known. From the calculation for each channel in Eq. (5), tristimulus value $\boldsymbol{t}$ can be formulated as:

$$\boldsymbol{t}=T_C^{-1}\begin{pmatrix} C_1 & 0 & 0\\ 0 & C_2 & 0\\ 0 & 0 & C_3\end{pmatrix}T_S\boldsymbol{p}\,, \tag{6}$$

where,

$$C_i=\frac{(T_{Ci,1}\ T_{Ci,2}\ T_{Ci,3})\begin{pmatrix}Z_r\\ Y_r\\ X_r\end{pmatrix}}{(T_{Si,1}\ T_{Si,2}\ T_{Si,3})\begin{pmatrix}B_r\\ G_r\\ R_r\end{pmatrix}}\,,\quad i=1,\,2,\,3\,. \tag{7}$$

In Eq. (7), $\boldsymbol{p}_r=(B_r\ G_r\ R_r)^t$ and $\boldsymbol{t}_r=(Z_r\ Y_r\ X_r)^t$ correspond to the sensor response and the tristimulus value of a reference reflectance, respectively, where t and −1 denote transpose and inverse matrix, respectively. Equation (6) is equivalent to the formula Eq. (17) in Ref. 14).

Drew and Finlayson estimated the sharpening matrix T_c using the Lagrange multiplier term and showed[14]:

$$T_C=\begin{pmatrix}0.50713 & -0.17050 & -0.08209\\ -0.37580 & 0.55150 & 0.04542\\ 0.02809 & -0.03359 & 0.26364\end{pmatrix}. \tag{8}$$

Their simulation results showed that the spectral sharpening matrix for an input device's sensitivities T_S is optimized when the sharpened color matching functions, $T_C X(\lambda)$, are projected onto the vector subspace spanned by the input device sensitivities[†]: $(T_S S(\lambda))^t = S(\lambda)^+ S(\lambda)(T_C X(\lambda))^t$, where $^+$ denotes pseudo inverse matrix[23] Therefore, T_S is given by

$$T_S = T_C X(\lambda) S^t(\lambda)(S(\lambda)S(\lambda)^t)^{-1}. \quad (9)$$

Using Eqs. (6) and (9) tristimulus values relative to a canonical illuminant can be obtained. CIE standard D65 illuminant was used as the canonical illuminant in the following.

3. Experimental Procedures and Results

3.1 Experimental Procedures

The same experimental procedures and data were used for the present study as described in Ref. 19). A CCD video camera (Sony DXC-930 with a standard zoom lens VCL-712BX) was used to capture the color images. Spectral sensitivities of the camera are presented in Fig. 1.[19] Figure 2 shows the sharpened color matching functions and the sharpened spectral sensitivities which were computed using the sharpening matrix of Eq. (9).

Macbeth color checker (24 colors), Kodak Q60R1 (228 colors) and offset (121 colors) color charts were used for the experiments. Illuminants used were outdoor light through a window, fluorescent lamps (National FLR 40S W/M-X) used for room illumination and SOLAX (Seric XC-100A), which is the light source simulating CIE D65 standard illuminant.

The color charts were placed on the wall of the room and were viewed in the normal direction. The outdoor lights through the window and the lights from eight fluorescent lamps hanging from the ceiling were used for the illumination; the illumination thus had various angles to the surface. The lights from the SOLAX, on the other hand, were illuminated at a fixed angle of about 45° to the surface normal. To measure the spectral radiant power distribution of an illuminant, the distribution of the light reflected on a surface with known spectral reflectance was measured by spectroradiometer (Minolta CS-1000). By dividing the spectral radiant power with surface reflectance element-wise, the distribution of an illuminant can be obtained. In the results, as represented in Fig. 3, the distribution of a reflected light was averaged over 10 nm since the spectral radiant power was measured at 1 nm intervals by the spectroradiometer.

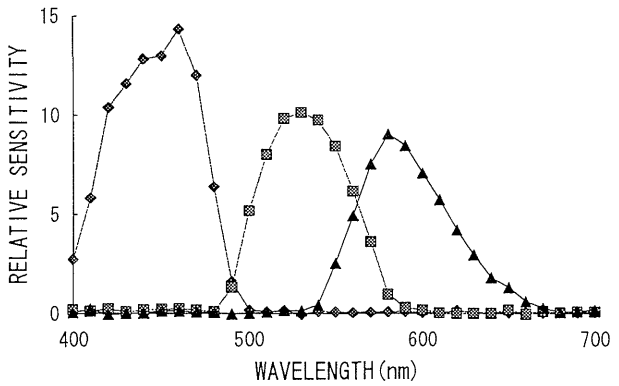

Fig. 1. Spectral sensitivities of the video camera (DXC-930).[19] ◆ blue, ■ green, ▲ red.

[†]Drew *et al.* wrote that the projection of input device sensitivities onto sharpened color matching function is the optimal sharpened sensitivities (p. 123 in Ref. 14). This sentence is not correct since if the sharpened sensitivities are the projection of spectral sensitivities onto sharpened color matching functions, as they stated, then the sharpened spectral sensitivities become a linear combination of color matching functions: therefore the left-hand side of Eq. (4) does not hold, that is, the sharpened sensitivities must be a linear combination of the sensitivities that are as close as possible to sharpened color matching functions.

The estimation was carried out for the projection of sensitivities of an input device onto the subspace spanned by sharpened color matching functions. The results were not accurate compared with the projection of sharpened color matching functions onto the subspace spanned by input device sensitivities. For example, 7.09 of ΔEab^* was obtained for subtracted data of Kodak Q60 under the outdoor illuminant in the projection of the sensitivities onto the sharpened color matching functions. Compare the results in Table 1.

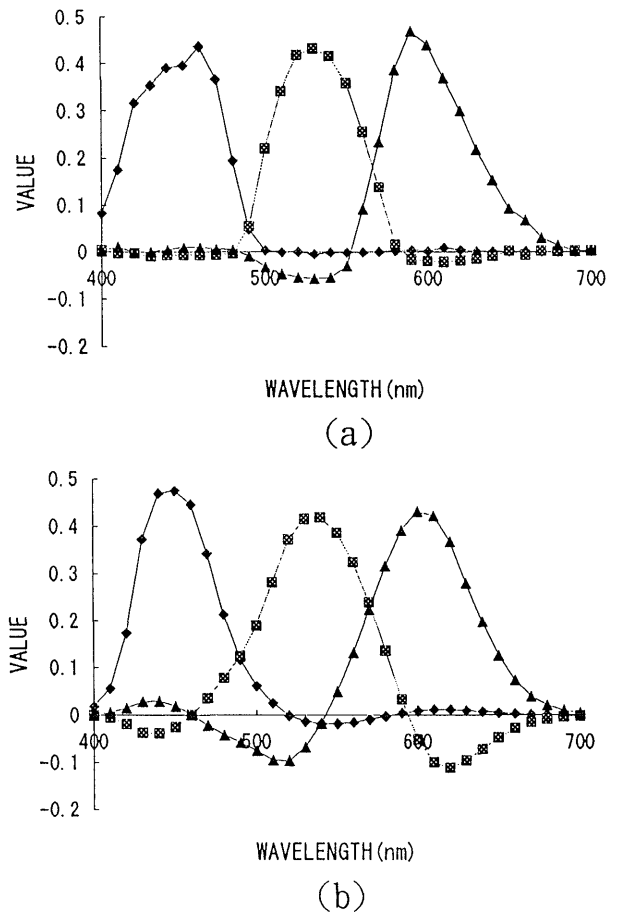

Fig. 2. Sharpened spectral sensitivities of the video camera (a), ◆ blue, ■ green, ▲ red. Sharpened color matching functions (b). ◆$\bar{z}(\lambda)$, ■$\bar{y}(\lambda)$, ▲$\bar{x}(\lambda)$.

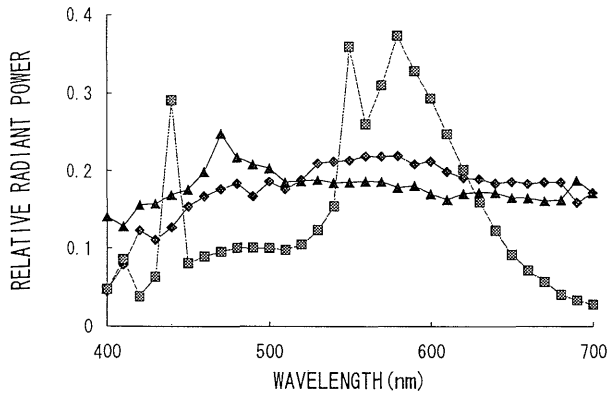

Fig. 3. Spectral radiant power distribution of the illuminants used in the experiments. ◆ Outdoor, ■ Fluorescent, ▲ SOLAX.

Image signals from the video camera were converted to 8 bits digital data by A/D converter and were stored in the frame memory. The dark signals were subtracted from the image data, and these are called actual image data below. The interface reflectance component at the glossy surface of a Kodak Q60R1 color chart, in the sense of dichromatic reflection model, influences the accuracy of the estimated colorimetric values.[19] For the lighting condition of SOLAX, the interface reflectance component by the glossy surface of Q60R1 is negligible due to the viewing geometry. For the outdoor and fluorescent illuminant, however, the interface reflectance component is not negligible since the illuminations are incident on the surface from various directions. The reflected light from a color with negligible body reflection, that is, a true black color, is considered the interface reflectance component. Therefore, minimum value of actual image data on a color chart which contains a black can be considered a signal by the interface reflectance component since the interface component is usually very small compared with the body reflection component in this viewing geometry. To reduce the interface reflectance component included in the actual image data, the minimum value of actual image data on a color chart was subtracted from that of each channel, which is called subtracted image data, in Kodak Q60R1. For Macbeth color checker and offset colors, actual image data were used for surface recovery since these color charts have no glossy surface.[19]

The reference reflectance $R_r(\lambda)$ used in this experiment was a color patch which looked like a white on each color chart, and the same color was used as a standard reflectance in the two computational models. Their spectral reflectance had been measured in advance by spectrophotometer (Minolta CM 2022) in the visible wavelength region between 400 to 700 nm at 10 nm intervals and were used to estimate colorimetric values. In the finite-dimensional linear model, the basis vectors for illuminants $E_i(\lambda)_{,i=1-3}$ were the first three obtained by singular value decomposition for mean, first and second characteristic vectors by Judd *et al.*[12] Basis vectors for surfaces $R_i(\lambda)_{,i=1-3}$ were derived from PCA on the data set of Kodak Q60 R1; those for illuminants and surfaces are presented in Fig. 1 of Ref. 18). The same set of basis vectors for daylight illuminants was used to express the three different illuminants, and the same set of basis vectors to represent surfaces was also used to recover the surface reflectances for three different color charts.

3.2 *Experimental Results*

The influence of the interface reflectance at the glossy surface of the Kodak Q60R1 color chart is summarized in Table 1. The values shown represent the average color differences ΔEab^* between estimated and actual colorimetric values in CIELAB color space using CIE 1931 standard observer under CIE standard D65 illuminant and standard deviations of ΔEab^* in parenthesis. A set of basis vectors of daylight illuminants was used for the estimation in the finite-dimensional linear model and the values of ΔEab^* in the linear model are the same data as used in Ref. 19). The values of ΔEab^* in the subtracted data are always smaller than those values of the actual data for two computational models under an outdoor and a fluorescent illuminants. The values of ΔEab^* under SOLAX for subtracted data are larger than those for actual image data. These results indicate that the interface reflectance component at the glossy surface influences the accuracy of the estimated colorimetric values. The values of ΔEab^* by the linear model are in all cases smaller than those by the spectral sharpening model.

The values of ΔEab^* estimated from subtracted image data were compared with those obtained by the computer simulations. Computer simulation was carried out using computed image data from the combination of the spectral sensitivities of the video camera, the spectral radiant power distribution of an illuminant and the surface spec-

Table 1. Influence of interface reflections on average color differences ΔEab^* in Kodak Q60R1 color chart.

Illuminant	Actual data[b]		Subtracted data[c]	
	Linear Model[a]	Sharpening	Linear Model[a]	Sharpening
Outdoor	8.12(6.22)[d]	10.09(6.84)	3.14(2.04)	4.28(2.68)
Fluorescent	8.44(6.28)	10.14(6.75)	5.63(3.42)	6.67(4.26)
SOLAX	3.57(1.98)	4.76(3.14)	4.79(3.66)	4.99(3.18)

[a]Basis vectors for daylight illuminant were used for the estimation.
[b]Actual data are defined as the image data derived from a subtraction of dark signals from the image data.
[c]Subtracted data are defined as the data derived from a subtraction of the minimum value of actual data from each actual image data to reduce an interface reflection component included in the actual data.
[d]The values in parenthesis indicate standard deviations.

Table 2. Average color difference ΔEab^* of estimated colorimetric values in CIELAB color space for Kodak Q60 under different illuminants.

Illuminant	Experimental Results		Simulation	
	Linear Model[a]	Sharpening	Linear Model[a]	Sharpening
Outdoor	3.14(2.04)[b]	4.28(2.68)	1.81(1.40)	3.76(3.00)
Fluorescent	5.63(3.42)	6.67(4.26)	4.53(2.87)	5.29(3.75)
SOLAX	4.79(3.66)	4.99(3.18)	1.57(1.27)	3.64(3.04)

[a]Basis vectors for daylight illuminants were used for the estimation.
[b]The values in parenthesis indicate standard deviations.

Table 3. Average color difference ΔEab^* of estimated colorimetric values in CIELAB color space for different media under different illuminants.

Medium	Linear Model[a]			Sharpening Model		
	Outdoor	Fluorescent	SOLAX	Outdoor	Fluorescent	SOLAX
Q60	3.14(2.04)	5.63(3.42)	4.79(3.66)[b]	4.28(2.68)	6.67(4.26)	4.99(3.18)
MCBETH	5.00(2.94)	7.76(4.64)	6.12(3.65)	5.95(4.47)	8.16(6.60)	6.75(3.53)
OFFSET	3.52(2.32)	6.55(4.60)	4.28(1.90)	7.18(4.41)	9.93(7.08)	4.98(2.50)

[a]A restricted set of basis vectors for daylight illuminant and basis vectors derived from PCA of Kodak Q60 were used to express the illuminants and surfaces, respectively.
[b]The values in parenthesis indicate standard deviation.

Table 4. Typical example of estimated color difference in CIELAB color space from image data of Macbeth color checker imaged under fluorescent lamp.

No.	Color Difference	
	Linear Model[a]	Sharpenig Model
1	8.64	10.03
2	4.57	6.71
3	4.27	3.55
4	6.63	4.58
5	5.44	3.30
6	4.96	9.04
7	14.09	16.18
8	8.95	5.35
9	9.26	15.13
10	9.83	10.00
11	6.53	5.23
12	14.56	16.39
13	6.69	2.03
14	4.22	3.46
15	21.03	26.52
16	10.53	11.06
17	12.09	16.15
18	12.52	15.63
19	1.52	0.00
20	2.83	1.44
21	2.88	1.72
22	2.74	2.24
23	4.18	3.68
24	7.18	6.31

[a]Basis functions for daylight illuminant and Kodak Q60R1 were used for the estimation in linear model.

tral reflectance of colors. The simulated values of ΔEab^* of 3.76, 5.29 and 3.64 of the spectral sharpening model are similar to those of 4.01 and 5.08 for the Munsell color chart by Drew *et al.*,[14] suggesting that the simulation of the present study is reasonable. The values from the experiment are always larger than those of simulations due to the noise included in image data in the two computational models, as discussed later.

The values of ΔEab^* of the linear model are smaller than those of the sharpening model in the experiments and simulations, although a restricted set of basis vectors for daylight illuminants was used.[18,19] This results is important since the restricted set of basis vectors of daylight illuminants can be used[18,19] for different illuminants and shows that the linear model has the same advantage as the spectral sharpening model, which does not use the finite-dimensional linear model.

The colorimetric values were estimated on the three different color charts under three different illuminants for two computational models. The same set of basis vectors for daylight illuminant was used to represent three different illuminants, and the same set of basis vectors for surfaces was used for the surface estimation in the linear model. The subtracted data for Kodak Q60R1 and actual data for Macbeth and offset were used for the estimations. The values of ΔEab^* are summarized in Table 3. Results of the linear model are always more accurate than those of the spectral sharpening model. The two models show media and illumination independence.

A typical example of color difference of the Macbeth color checker is represented in Table 4 using image data under fluorescent lamp for the two models, where basis functions for daylight illuminants and Kodak Q60R1 were used for the estimation. As seen, the color difference of the reference reflectance (No. 19) is zero in the sharpening model, as expected from Eq. (3), but the maximum value and average color difference, as listed in Table 3, are larger than the linear model.

4. Discussion

Thus the experimental and simulated results on the estimation of colorimetric values, show the finite-dimensional linear model to be more accurate than the spectral sharpening model. The sharpened spectral sensitivities and color matching functions are not consistent with the delta-functions as seen in Fig. 2 of the present paper or in Fig. 1 of Ref. 14). Therefore, the invariance of the ratio of the sharpened sensor's response of a surface to that of a reference reflectance with changes in illuminant, as shown by Eq. (4), does not hold exactly but is only an approximation. This would be the main reason for the inaccuracy of the spectral sharpening model. The optimization of the sharpened sensitivities of a camera for colors of some media and for some illuminants may improve the accuracy as mentioned by Drew and Finlayson,[14] but this optimization diminishes the advantage of media and illuminant independence of this model. The values of ΔEab^* for fluorescent lamp were large in both cases, i.e., in these experimental and simulated results, for both computational models. This causes one to believe that the estimation accuracy would be reduced under fluorescent lamp including the sharp spectral lines. However, the values of ΔEab^* are 3 units below in the fluorescent lamp recommended for calculating CIE index of metamerism such as F2 and F3 in the simulation results by the linear model.[18]

This model may be used for some kind of fluorescent lamps. Although the simulation results in the finite-dimensional linear model are promising for outdoor and SOLAX illuminants, the experimental results are insufficient. The degradation of the estimation accuracy is due to the noises included in image data. The estimation errors in the spectral sensitivities, the circuit noise, the quantization errors, the flare lights included in the detected lights and the non-uniformity of the illumination's intensities over the color chart may be sources of the data noise. The non-uniformity of the illumination was the most important factor degrading the accuracy since the intentional non-uniform illuminations by SOLAX reduced the accuracy. The second factor influencing the accuracy may be the estimation errors for the interface reflectance component included in reflected lights at the surfaces of object colors as given in Table 1. An appropriate method to separate interface reflectance components included in the reflected lights at an object's surface will improve the estimation accuracy.

The spectral radiant power distributions of outdoor illuminants might have changed slightly during the image acquisition for the three color charts, although the procedure was performed immediately. Since the same image data were used for the two models, the compared results for each color chart are not influenced by the change.

For quantitative evaluation of the estimated colorimetric values, an interface reflectance component included in the image data was excluded, that is, only the body reflection components were used to calculate the colorimetric values in this study. The separation of image signals into body and interface reflection components may not be suitable for color reproduction, since an interface component at a glossy object must be reproduced as an image. However, a spectral reflectance distribution which includes an interface reflectance component depends on the geometric conditions of the illumination, the object and viewing angle of the camera. Evaluation must therefore be performed based on standard geometric conditions and objects at the scene.

5. Conclusions

An experiment was performed to estimate colorimetric values through the use of image data captured by video camera under different illuminants using a reference reflectance with known surface spectral reflectance. The accuracy was compared for two computational color constancy models, the finite-dimensional linear model and the spectral sharpening model, and it was confirmed that the two models do not require prior knowledge of surfaces and illuminants. The finite-dimensional linear model gives the more accurate results in simulations and experiments. A uniform intensity of illumination over a scene and correct estimation of interface reflectance component included in the reflected light are important to obtain accurate estimation results.

References

1) Po-Chieh Hung: Proc. SPIE **1448** (1991) 164.
2) H.R. Kang: J. Imaging Sci. Technol. **36** (1992) 162.
3) S.A. Rajala, H.J. Trussel and A.P. Kakodkar: Proc. SPIE **2170** (1994) 53.
4) J.M. Kasson, S.I. Nin, W. Plouffe and J.L. Hafner: J. Electron. Imaging **4** (1995) 226.
5) L.T. Maloney and B.A. Wandell: J. Opt. Soc. Am. A **3** (1986) 29.
6) J. Ho, B.V. Funt and M.S. Drew: IEEE Trans. Pattern Anal. Mach. Intell. **PAMI-12** (1990) 966.
7) M. D'Zmura and G. Iverson: J. Opt. Soc. Am. A **10** (1993) 2148.
8) M. D'Zmura and G. Iverson: J. Opt. Soc. Am. A **10** (1993) 2166.
9) J. Cohen: Psychon. Sci. **1** (1964) 369.
10) J.P.S. Parkkinen, J. Hallikainen and T. Jaaskelainen: J. Opt. Soc. Am. A **6** (1989) 318.
11) L.T. Maloney: J. Opt. Soc. Am. A **3** (1986) 1673.
12) D.B. Judd, D.L. MacAdam and G. Wyszecki: J. Opt. Soc. Am. **54** (1964) 1031.
13) G.D. Finlayson, M.S. Drew and B.V. Funt: J. Opt. Soc. Am. A **11** (1994) 1553.
14) M.S. Drew and G.D. Finlayson: IS&T and SID's 2nd Color Imaging Conf. (1994) 121.
15) G. Buchsbaum: J. Frank. Inst. **310** (1980) 1.
16) M.H. Brill: J Theor. Biol. **71** (1978) 473.
17) C.L. Novak and S.A. Shafer: Proc. SPIE **1453** (1991) 353.
18) N. Shimano: Opt. Rev. **4** (1997) 358.
19) N. Shimano: Opt. Rev. **4** (1997) 707.
20) S.A. Shafer: Color Res. Appl. **10** (1985) 210.
21) S. Tominaga: Color Res. Appl. **19** (1994) 277.
22) J.L. Dannemiller: J. Opt. Soc. Am. A **9** (1992) 507.
23) B. Noble and J.W. Daniel: *Applied Linear Algebra* (Prentice-Hall, Englewood Cliffs, 1998) 3rd ed., p. 348.